The EMBO Journal Vol. 22 No. 3 pp. 494–501, 2003

Structural basis for recruitment of glycogen synthase kinase 3β to the axin–APC scaffold complex

Rana Dajani[1], Elizabeth Fraser[2], S.Mark Roe[1], Maggie Yeo[2], Valerie M.Good[1], Vivienne Thompson[1], Trevor C.Dale[2] and Laurence H.Pearl[1,3]

[1]Section of Structural Biology and [2]Cancer Research UK Centre for Cell and Molecular Biology, Institute of Cancer Research, Chester Beatty Laboratories, 237 Fulham Road, London SW3 6JB, UK

[3]Corresponding author
e-mail: l.pearl@icr.ac.uk

Glycogen synthase kinase 3β (GSK3β) is a serine/threonine kinase involved in insulin, growth factor and Wnt signalling. In Wnt signalling, GSK3β is recruited to a multiprotein complex via interaction with axin, where it hyperphosphorylates β-catenin, marking it for ubiquitylation and destruction. We have now determined the crystal structure of GSK3β in complex with a minimal GSK3β-binding segment of axin, at 2.4 Å resolution. The structure confirms the co-localization of the binding sites for axin and FRAT in the C-terminal domain of GSK3β, but reveals significant differences in the interactions made by axin and FRAT, mediated by conformational plasticity of the 285–299 loop in GSK3β. Detailed comparison of the axin and FRAT GSK3β complexes allows the generation of highly specific mutations, which abrogate binding of one or the other. Quantitative analysis suggests that the interaction of GSK3β with the axin scaffold enhances phosphorylation of β-catenin by >20 000-fold.

Keywords: β-catenin/insulin signalling/phosphorylation/signal transduction/Wnt signalling

Introduction

Glycogen synthase kinase 3β (GSK3β) plays a key role in Wnt signalling, hyperphosphorylating the transcriptional co-activator β-catenin, and thereby promoting its ubiquitylation and targeted destruction (Ding and Dale, 2002). In this role, GSK3β is recruited to a multiprotein complex based on the adenomatous polyposis coli protein (APC), via its interaction with the scaffold protein axin (also known as conductin) (Behrens *et al*., 1998; Hart *et al*., 1998; Ikeda *et al*., 1998). As well as GSK3β, axin also provides binding sites for the β-catenin substrate, and for the α-isoform of casein kinase I (CKIα), which phosphorylates β-catenin on Ser45 and 'primes' the sequential phosphorylation of Thr41, Ser37, Ser33 and Ser29 by GSK3β (Liu *et al*., 2002). Mutations in components of this system that prevent β-catenin hyperphosphorylation by GSK3β are strongly associated with cancers (Polakis, 2000), through inappropriate activation of proliferative genes such as c-*myc* by elevated β-catenin levels (He *et al*., 1998).

Wnt signalling through the Frizzled receptor and mediated by Dishevelled, acts to inhibit β-catenin hyperphosphorylation by GSK3β, although the details of this are not well understood (Wodarz and Nusse, 1998). One possible mechanism involves FRAT1/GBP (Yost *et al*., 1998) which binds to Dishevelled (Li *et al*., 1999), and to GSK3β in competition with axin, thereby displacing it from the axin–APC complex and preventing its access to β-catenin. Direct competition between axin and FRAT1/GBP-derived peptides has been demonstrated biochemically (Thomas *et al*., 1999), and overlapping binding sites for axin and FRAT1/GBP on the structure of GSK3β (Dajani *et al*., 2001) have been mapped genetically (Ferkey and Kimelman, 2002; Fraser *et al*., 2002). The detailed binding interactions made by FRAT1 have been defined by a crystal structure of a complex between GSK3β, phosphorylated on Tyr216, and a 39 residue FRAT1-derived peptide (Bax *et al*., 2001). We now describe the crystal structure of pTyr216-GSK3β bound to a 19 residue, minimal GSK3β-binding peptide derived from axin. The structure of the complex confirms the partial overlap of the binding sites of axin and FRAT1/GBP predicted from genetic and biochemical studies, but reveals significant differences in the detailed interactions, and identifies key residues mediating the differential interaction with axin and FRAT.

Results

Activation segment phosphorylation

The crystal structure of the (pTyr216)-GSK3β–axin(383–401) complex was determined by molecular replacement using the structure of unphosphorylated GSK3β (Dajani *et al*., 2001), and refined at 2.4 Å resolution (see Materials and methods). Overall, the phosphorylated and axin-bound structure is very similar to that of the unphosphorylated enzyme, with the exception of the activation segment (212–220) and the loop from 285–299 (see below). Clear difference density for a phosphorylated Tyr216 is visible, and indicates a substantial movement of the side chain from its position in the unphosphorylated structure to interact via the phosphate with the side chains of Arg220 and Arg223 as predicted (Dajani *et al*., 2001) (Figure 1A and B). Apart from the change in rotamer of Tyr216, the conformation of the activation loop is unchanged from the activated conformation observed in the unphosphorylated structure, in stark contrast to the structurally related mitogen-activated protein (MAP) kinases (Canagarajah *et al*., 1997). The role of Tyr216 phosphorylation in GSK3β function has been uncertain, with contradictory results from *in vivo* studies (Itoh *et al*., 1995; Murai *et al*., 1996). To gain some

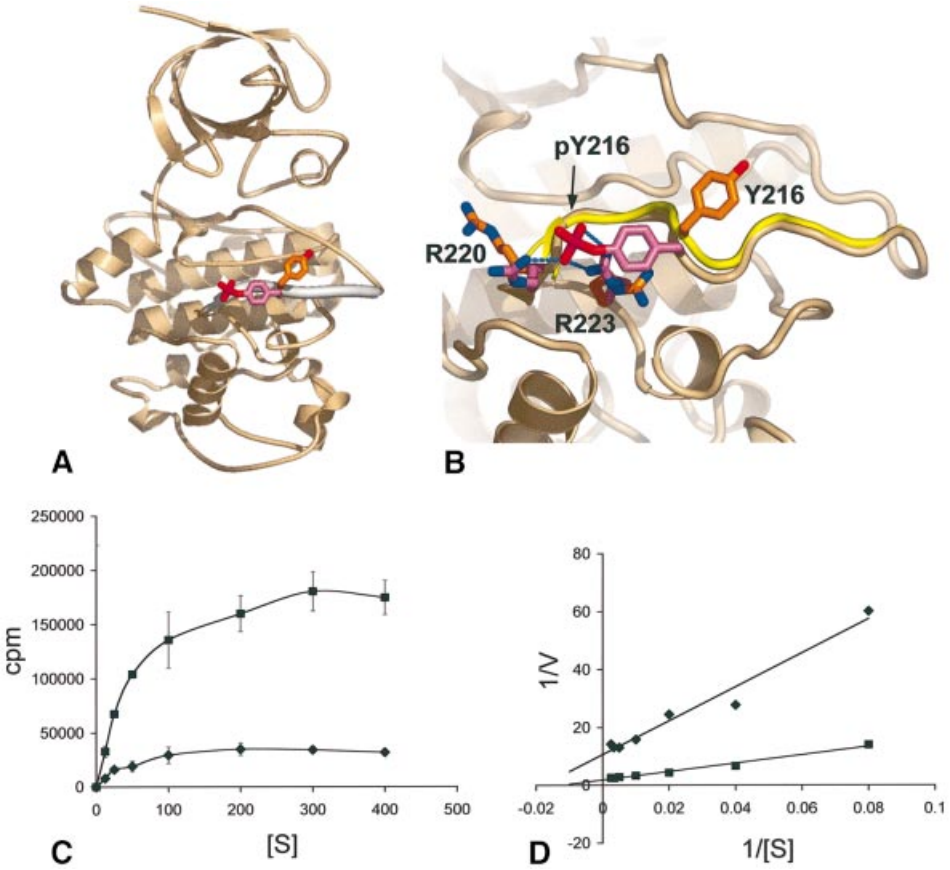

Fig. 1. Structural and biochemical consequences of Tyr216 phosphorylation. (**A**) Secondary structure cartoon of GSK3β showing the activation segment (thickened) and the conformations of Tyr216 in the unphosphorylated protein (orange and red) and pTyr216 in the present structure (pink and red). (**B**) Comparison of the activation segment in the Tyr216 phosphorylated (buff and pink) and unphosphorylated conformations (yellow and orange). Phosphorylation causes an ~120° rotation of the tyrosine side chain and repositioning of the side chains of Arg220 and Arg223, to hydrogen bond to the phosphate group of pTyr 216. (**C**) Kinase activity of unphosphorylated (diamonds) and pTyr 216 (squares) GSK3β on a phospho-primed peptide substrate as a function of peptide substrate concentration. All points are the means of three measurements. (**D**) Double reciprocal plot of the data from (C). For the unphosphorylated GSK3β, K_m = 60 μM, k_{cat} = 0.7; for pTyr216 phosphorylated GSK3β, K_m = 85 μM, k_{cat} = 3.7. pTyr216 phosphorylation causes an ~5-fold increase in activity.

quantitative insight into the effect of Tyr216 phosphorylation, we compared the kinase activity of GSK3β with or without Tyr216 phosphorylation against a phospho-primed peptide substrate (Figure 1C and D). We observed a clear stimulatory effect of Tyr216 phosphorylation on GSK3β activity, but only ~5-fold that of the unphosphorylated enzyme. This is a very modest effect in comparison with related kinases, where activation segment tyrosine phosphorylation produces >1000-fold stimulation, and suggests that this phosphorylation has a modulatory, rather than a directly regulatory role in GSK3β function. Tyr216 phosphorylation had its major effect on the k_{cat} of the reaction rather than the K_m, consistent with decreased affinity of the phosphorylated enzyme for the more negatively charged phosphorylated product, rather than an increased affinity for the substrate.

Axin-binding site

The axin-derived 19 residue peptide binds as a single amphipathic α-helix, into a hydrophobic surface channel on the C-terminal helical domain (Figure 2A and B). Only the central 17 residues of the peptide are visible in the electron density, suggesting that the entire binding site has been occupied. The axin-binding channel is formed by an α-helix (262–273), and an extended loop from 285–299 which was poorly ordered in the unphosphorylated GSK3β structure (Dajani *et al*., 2001) but is well defined in the axin–peptide complex. On one wall of the channel, a hydrophobic helical ridge formed by axin residues Phe388, Leu392, Leu396 and Val399 packs into a helical groove formed by Val263, Leu266, Val267 and Ile270 of GSK3β (Figure 3A and B). On the opposite wall of the channel Pro385, Ala389, Ile393 and Leu396 of axin pack against Tyr288, Phe291, Phe293, Pro294 and Ile296 from the extended GSK3β loop. The base of the channel at the N-terminal end of the axin peptide is formed by the side chains of Ile228 and Phe229, which pack against the side chain of Phe388. In addition to the substantial hydrophobic interface, there are a few polar side chain interactions: Arg395 of the axin peptide makes hydrogen bonding and ionic interactions with Asp264, and Gln400 hydrogen bonds to the peptide carbonyl of Gln295 of GSK3β. The bound axin overlaps the position of part of the second GSK3β molecule in the dimer observed in the crystals of

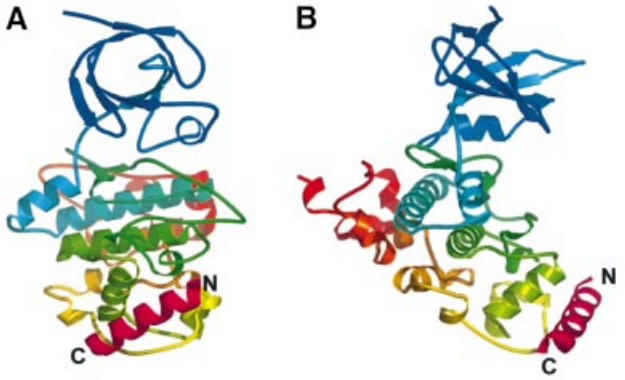

Fig. 2. C-terminal axin-binding site. (**A**) Secondary structure cartoon of GSK3β (colour-ramped blue to red from the N- to the C-terminus) with the bound axin(383–401) peptide (magenta). (**B**) As (A), but rotated 90° around the vertical.

uncomplexed GSK3β (Dajani *et al*., 2001), and explains the observed ability of axin to disrupt GSK3β dimers in solution (Fraser *et al*., 2002).

Comparison of axin and FRAT binding

A great deal of evidence points to a substantive co-localization of the axin- and FRAT-binding sites on GSK3β, so that their binding is mutually competitive (Thomas *et al*., 1999) and the majority of mutations that impair the binding of one similarly affect the other (Ferkey and Kimelman, 2002; Fraser *et al*., 2002). This has now been confirmed at the molecular level by the structure presented here, and the structure of a GSK3β–FRAT peptide complex (Bax *et al*., 2001). For both axin and FRAT-derived peptides, the major binding site is provided by the channel between the helix (262–273) and the extended loop (285–299), which effectively is 'induced' by peptide binding. In both cases, there is a hydrophobic helix–helix ridge–groove interaction involving residues Val263, Leu266, Val267 and Ile270 of GSK3β and helically disposed residues from the ligand peptide. In the FRAT complex, this hydrophobic ridge is provided by residues Leu212, Ala216 and Leu220, and, on the basis of that structure, a similar binding mode for an axin-derived peptide was proposed (Bax *et al*., 2001), in which the corresponding interactions would be provided by Leu392, Leu396 and Val399 of axin. It is clear from the GSK3β–axin peptide complex presented here that while the proposal of a helical binding mode for the axin peptide was correct, the identification of corresponding residues was incorrect and misaligned by a complete helical turn. Thus, the residues in axin corresponding approximately to Leu212, Ala216 and Leu220 of FRAT are in fact Phe388, Leu392 and Leu396.

The most significant difference in the binding of the axin and FRAT peptides is the presence of a sharp turn in the FRAT peptide, which breaks its structure into two distinct and separate α-helical segments, while the axin peptide is a single unbroken α-helix (Figure 4A). The 'breakpoint' in the FRAT peptide occurs at Gly210–Asn211, exposing the peptide NH groups of Leu212, Ile213 and Lys214 at the N-terminus of the second helical segment, which then donate hydrogen bonds to the side chains of Tyr288 and Glu290 from the

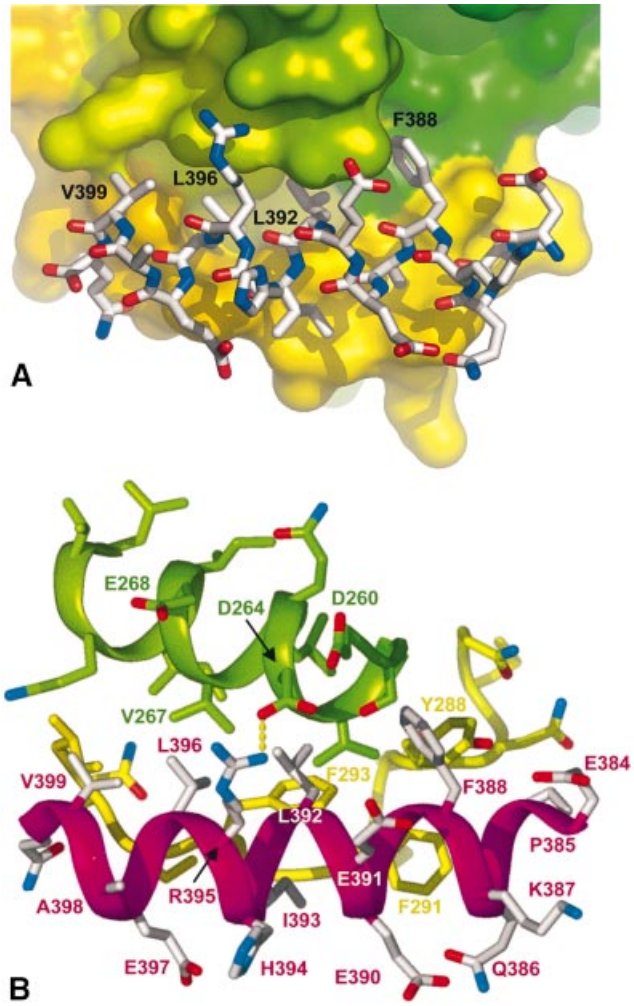

Fig. 3. Axin–GSK3β interactions. (**A**) Axin residues Phe388, Leu392, Leu396 and Val399 form a hydrophobic helical 'ridge' that packs into a hydrophobic groove formed between helix 262–273 (green surface) and the extended loop from 285–299 (yellow surface) in GSK3β. (**B**) The axin(383–401) peptide (magenta and white) makes only a single side chain hydrogen bond to GSK3β (green-yellow), from Arg395 to Asp264.

extended loop in GSK3β. The positions corresponding to Gly210 and Asn211 in the axin peptide are occupied by Gln386 and Lys387, which remain fully hydrogen bonded in the helix, extending its length by a full turn compared with FRAT. Consequently, Tyr288 and Glu290 occupy quite different positions in the axin complex, compared with the FRAT complex, with the phenol ring of Tyr288 involved in hydrophobic interactions with Pro385 and Phe388 at the N-terminus of the axin helix, while Glu290 is fully exposed on the protein surface and free from any interactions (Figure 4B). The differential role of these residues in axin and FRAT binding indicated by the structural data was confirmed in an *in vitro* immunoprecipitation assay (see Materials and methods). Thus, Tyr288Phe or Glu290Gln mutations in GSK3β produced substantial reductions in FRAT binding compared with wild-type, with almost no effect on axin binding (Table I). While some residues in the 285–299 loop, such as Glu290, play no role in axin binding, others, such as Phe291 and Phe293, are involved in binding both axin and FRAT, but in quite different ways. In the axin complex, Phe291 is directed inwards, with the face of the phenyl ring packing

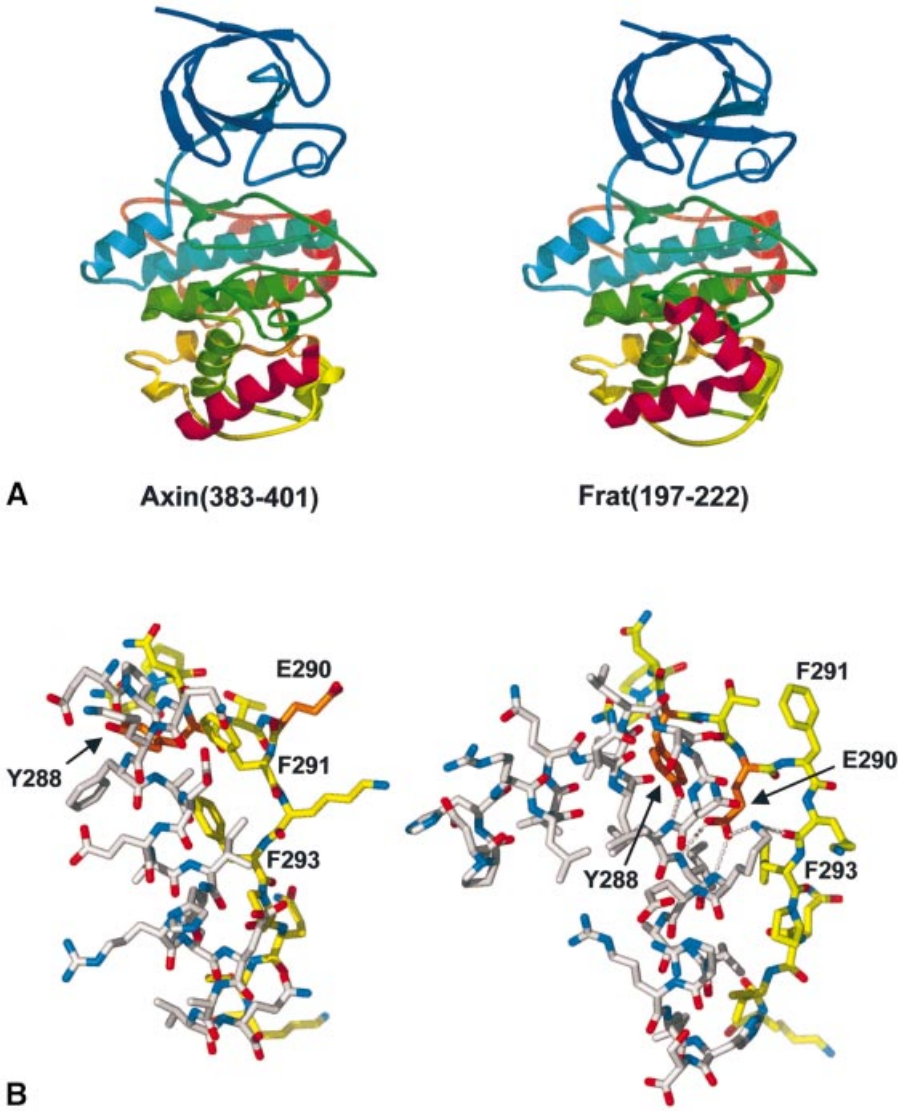

Fig. 4. Comparison of axin and FRAT binding to GSK3β. (**A**) The binding sites for the axin(383–401) peptide and FRAT(197–222) peptides are co-localized in the C-terminal domain of GSK3β. However, the two peptide have no sequence homology, and bind with different conformations and interactions. (**B**) The extended loop formed by residues 285–299 of GSK3β (yellow) adopts different conformations in binding axin and FRAT. In particular, residues Tyr288, Glu290 (orange), Phe291 and Phe293 adopt radically different conformations and interactions in the two complexes.

against Ala380 of axin. In the FRAT complex, Phe291 makes no direct contact with FRAT residues, but instead packs against Val289 of GSK3β, stabilizing a backbone conformation that swings the intervening residue Glu290 inwards to hydrogen-bond with the FRAT main chain. We found that a Phe291Leu mutation reduced binding to either ligand significantly, although only axin binding was significantly affected by a similar mutation in a study using *Xenopus* GSK3β and GBP (Ferkey and Kimelman, 2002). The side chain of Phe293 packs edge on into a hydrophobic depression formed by the side chains of Ala389, Leu392, Ile393 and Leu396 on the axin helix. In the FRAT complex, the side chain of Phe293 is rotated by 90° to pack against the side chain of Ile213. As would be expected, mutation of Phe293 diminishes binding to both ligand proteins, but more so with axin, reflecting the more substantial interaction.

We had shown previously that a mutation in murine axin, equivalent to Leu392Pro in the human axin sequence used here, abolished binding to GSK3β (Smalley *et al.*, 1999). On the basis of the GSK3β–FRAT crystal structure, this effect was explained in terms of loss of a predicted hydrogen bond interaction between Tyr288 and the peptide nitrogen of residue 392, comparable with the interaction with Leu212 at the 'breakpoint' turn between the two helices in FRAT. However, it is clear from the present structure that unlike FRAT, the axin peptide does not break and Leu392 is fully hydrogen bonded in the continuous α-helix. The side chain of axin Leu392 is buried in a hydrophobic pocket formed by the side chains of Val263, Leu266, Val267 and Ile270 from the hydrophobic helix (262–273) on one side, and Phe293 from the extended loop in GSK3β on the other side. Mutation to the smaller proline would generate a packing defect in this extensive hydrophobic interface with GSK3β, and would disrupt the hydrogen bonding in the axin helix. The combination of these effects would be more than sufficient to abrogate axin binding.

Table I. Effects of GSK3β mutations on immunoprecipitation of axin and FRAT

Residue	Mutation	Axin binding (%)	Axin contacts	FRAT binding (%)	FRAT contacts
Y216	F	40	None	40	H200
Y216	E	100	None	100	H200
I228	K	5	F388	5	L203, L212
F229	Q	5	F388, L392	5	L212, I213
F229	A	10	F388, l392	5	L212, I213
V263	G	30	F388, E391, L392, R395	10	L203, L206, R219
L266	G	10	F388, L392	15	L212, A216
V267	G	0	L392, R395, L396, V399	100	A216, L220
I270	K	10	L392, L396	20	A216, L220
I270	G	0	None	0	A216, L220
I281	G	5	None	10	I213
N285	E	20	None	30	None
N285	D	25	None	50	None
Y288	R	5	P385, F388	10	V207, G210, N211, L212
Y288	F	100	P385, F388	20	V207, G210, N211, L212
Y288	A	70	P385, F388	5	V207, G210, N211, L212
E290	M	40	None	30	G210, N211, L212, I213, K214
E290	Q	100	None	10	G210, N211, L212, I213, K214
E290	D	80	None	10	G210, N211, L212, I213, K214
E290	K	80	None	40	G210, N211, L212, I213, K214
F291	L	10	Q386, A389	10	None
F293	A	5	A389, L392, I393, L396	20	I213
F293	Q	5	A389, L392, I393, L396	20	I213
I296	G	0	L396, Q400	20	V217, L220, H221
I296	T	0	L396, Q400	15	V217, L220, H221

At the C-terminal end of the common helical-binding channel, Val267 of GSK3β packs into a hydrophobic hole formed by the side chains of Leu392, Leu396, Val399 and Arg395 of axin, whose head group is positioned by a hydrogen bond to Asp264 of GSK3β. In an earlier mutagenesis study, a GSK3β Val267Gly/Glu268Arg mutant was the only one identified which displayed a significant reduction in axin but not FRAT binding (Fraser *et al*., 2002). We subsequently found that the GSK3β Val267Gly mutation alone is sufficient to abolish axin binding (Table I), presumably by generating a packing defect in the same hydrophobic interface disrupted by the axin Leu392Pro mutation (see above). While FRAT also contacts Val267, the FRAT helix at this point is in a 3_{10} conformation and makes a much less intimate interaction, so that loss of the valine side chain is significantly less disruptive.

Contribution of axin scaffold to β-catenin phosphorylation

Two major factors influence the rate of N-terminal β-catenin phosphorylation. These are the axin-dependent scaffolding of casein kinase 1, GSK3β and β-catenin, and the phospho-priming of the β-catenin substrate at Ser45 by casein kinase 1 (Liu *et al*., 2002; Yanagawa *et al*., 2002). Studies with glycogen synthase peptide substrates showed that phospho-priming enhanced GSK3β activity 400-fold (Harwood, 2001). Our studies with β-catenin peptides showed that phospho-priming enhanced GSK3β-dependent phosphorylation 30-fold (data not shown). To assess the enhancement of GSK3β activity by scaffolding, we compared the efficiency of β-catenin phosphorylation by GSK3β in free solution with that in an axin-scaffolded complex (Figure 5). To derive accurate figures, unbound β-catenin had to be separated from the axin–β-catenin complex to allow accurate estimates of the total levels of bound β-catenin. Based on these data, a scaffolding enhancement of 24 000-fold was calculated. Similar results were found by immunoblotting for phospho-β-catenin residues Thr41/Ser45 or by detection of radiolabelled γ-phosphate incorporation into β-catenin (data not shown).

For GSK3β, a combination of phospho-priming and scaffolding may thus be expected to enhance the proportion of N-terminal phosphorylated β-catenin, relative to free unphosphorylated β-catenin, by 720 000-fold ($30 \times 24\,000$). Although the effective *in vivo* concentrations of β-catenin, axin, GSK3β and CK1α are unknown, our data are consistent with a very substantial contribution of scaffolding to the efficiency of N-terminal hyperphosphorylation of β-catenin by GSK3β in the axin–APC complex.

Discussion

As predicted from mutagenesis studies (Ferkey and Kimelman, 2002; Fraser *et al*., 2002), the primary binding sites for axin and FRAT on GSK3β have been found to overlap substantially in the crystal structures, so that their binding is mutually exclusive. Despite this, the GSK3β-interacting regions of FRAT and axin show negligible sequence similarity and, although both are primarily helical, their detailed structures and interactions with GSK3β have substantial differences. This ability of GSK3β to bind two different proteins with high specificity via the same binding site is mediated by the conformational plasticity of the 285–299 loop. In the unliganded structure (Dajani *et al*., 2001), this loop is highly mobile

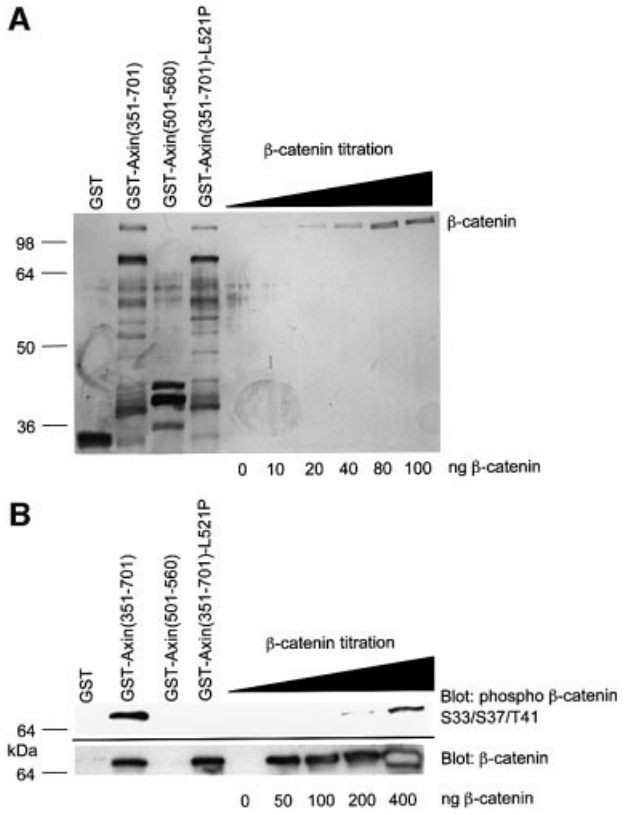

Fig. 5. Templating factor for axin phosphorylation of β-catenin. (**A**) Estimation of levels of axin-bound, β-catenin levels. A 3 μg aliquot of His-tagged β-catenin was incubated with the molar equivalent of each GST protein and precipitated with glutathione–Sepharose beads. A one-fifth equivalent of the washed beads was analysed by SDS–PAGE and silver stained. GSTAx-(351–701) is the central region of axin which encompasses both the β-catenin- and GSK3β-binding sites. The L521P mutation prevents GSK3β binding (Smalley *et al*., 1999). GSTAx-(501–560) is the GSK3β-binding domain alone. (**B**) Kinase assay. GSK3β (10 μM final concentration) was added to beads with bound GST proteins as shown in (A) or to increasing concentrations of free β-catenin under kinase assay conditions. Samples were analysed by SDS–PAGE and immunoblotting. GSTAx-(351–701) and GSTAx-(351–701)-L521P were normalized for β-catenin levels (2-fold increase in loading of the latter). Comparison of the levels of N-terminal phosphorylation of the β-catenin were made using an anti-phospho β-catenin Ser33/37 Thr41 antibody by timed autoradiographic exposures. Calculation: comparisons of phospho-β-catenin levels in lane 2 were made with comparable levels in the β-catenin titration. These were then normalized to the total level of β-catenin present, resulting in an estimate of a 40-fold molar excess of phospho-β-catenin S33/37/T41 in the presence of axin compared with that in free solution. To derive the scaffolding factor, this figure was multiplied by 3 (since only 1 in 3 axin molecules was estimated to bind a β-catenin; see A, track 2) and by 200 to compensate for the proportion of templates containing GSK3β [since GSK3β was added at a final concentration of 10 μM while GST–axin(368–701) was present at 2 μM]. The calculated scaffolding factor was consistent with additional assays in which the axin–β-catenin complex was double purified to remove unbound axin and β-catenin (data not shown).

and poorly defined, but is induced into one of two distinct and well-ordered structures that are specific to the individual ligand bound. Interestingly, the segments in Cdk2 topologically equivalent to the axin- and FRAT-binding segments in GSK3β are involved in interactions with the regulatory protein Csk1 (Bourne *et al*., 1996) and with KAP phosphatase (Song *et al*., 2001). However, these are less penetrating interactions than that of GSK3β with axin and FRAT, and the structure of the binding site on Cdk2 is essentially identical in both cases. While some residues in this versatile binding site in GSK3β are involved in interactions with both axin and FRAT, others are involved uniquely with one or the other, and their mutation now provides the opportunity for highly specific 'knockouts' that will help deconvolute the roles of FRAT and axin in Wnt signalling.

GSK3β achieves the clever trick of transducing signals for two completely independent pathways without any obvious cross-talk or interference. At least in its Wnt signalling role, a substantial part of this insulation is achieved by the recruitment of a subset of the cellular GSK3β pool into a multiprotein complex that brings GSK3β and its β-catenin substrate into close proximity. Although the true biological role of FRAT in Wnt signalling is not yet fully understood, its association with Dishevelled and its ability to compete with axin for binding to GSK3β is strong circumstantial evidence for its direct involvement in 'inhibiting' β-catenin phosphorylation by GSK3β. Inhibition of GSK3β via insulin or growth factor signalling pathways operates by a completely different mechanism in which the N-terminus of GSK3β is converted to an autoinhibitory pseudo-substrate via phosphorylation of Ser9 (Dajani *et al*., 2001; Frame *et al*., 2001). Functional segregation of the insulin/growth factor and Wnt roles requires either that there is no exchange between the subsets of the cellular GSK3β pool committed to each role, or that the recruitment of GSK3β to the axin–APC complex can reverse or override inhibitory Ser9 phosphorylation present on a recruited GSK3β molecule. Phosphatases capable of removing extant Ser9 phosphorylation are certainly known to be associated with the axin–APC complex (Hsu *et al*., 1999; Seeling *et al*., 1999). Alternatively, the very substantial enhancement in activity towards β-catenin afforded by the axin 'scaffolding' may simply allow a primed β-catenin substrate to out-compete a pSer9–GSK3β N-terminal peptide for access to the substrate-binding site.

Table II. Crystallographic statistics

	All data (outer shell)
Data collection	
R_{merge}	0.076 (0.305)
$I/\sigma(I)$	6.9 (2.2)
Completeness (%)	98.9 (99.7)
Multiplicity	6.8 (3.9)
No. of unique reflections	22 740 (3252)
Structure refinement	
No. of atoms (protein)	2942
No. of atoms (all)	3086
Resolution range	20.0–2.4 Å
R_{cryst}	0.233
R_{free}	0.260

Materials and methods

Expression and purification

Human GSK3β was cloned, and expressed in the Bac-to-Bac baculovirus expression system (Life Technologies), as previously described (Dajani *et al*., 2001). Frozen cells from a 5 l culture were lysed by thawing, and hand homogenizing on ice in buffer A (50 mM HEPES–NaOH pH 7.5, 300 mM NaCl, 50 mM NaF and 1 mM Na orthovanadate, supplemented

with protease inhibitors). The cell extract was centrifuged (48 000 *g* for 60 min at 4°C) and the clarified supernatant was mixed with 10 ml of Talon metal affinity resin (Clontech) for 2 h at 4°C. The resin was pelleted by centrifugation at 700 *g* for 3 min at 4°C, packed into an XK 16/20 column (Amersham Biosciences), and washed with 20 column volumes of buffer A and 20 column volumes of buffer A + 5 mM imidazole. The protein was eluted with 50 mM HEPES-NaOH pH 7.0, 300 mM NaCl, 200 mM imidazole, 50 mM NaF and 1 mM Na orthovanadate. EDTA (2 mM) and dithiothreitol (DTT; 2 mM) were added to the eluted protein, which was then incubated overnight at 4°C with ~3 mg (or 20 000 U) of rTEV protease, to remove the histidine tag. The protein was concentrated to 15 ml using a Vivaspin 20 ml centrifugal concentrator (Vivascience), and desalted (HiPrep 26/10 desalting column, Amersham Biosciences) in 50 mM HEPES–NaOH pH 7.0 and 300 mM NaCl. The protein was mixed with 10 ml of Talon for 2 h at 4°C to separate cleaved GSK3β from non-cleaved protein, rTEV protease and other contaminants. EDTA (1 mM) and DTT (1 mM) were added to the protein, which was concentrated and diluted in ion exchange buffer A (25 mM HEPES–NaOH pH 7.0 and 1 mM DTT) to obtain an NaCl concentration of 50 mM. The protein was applied to an 8 ml Source 15S column, HR 10/10 (Amersham Biosciences). The resin was washed with buffer A and the protein was eluted with a gradient of 0–500 mM NaCl over 50 column volumes in 25 mM HEPES–NaOH pH 7.0 and 1 mM DTT. The protein was concentrated to ~10 mg/ml using a 2 ml Centricon centrifugal concentrator (Amicon), and the purified GSK3β was stored at –80°C. Western blot analysis confirmed the protein to be tyrosine phosphorylated.

Crystallography

Samples of the phosphorylated GSK3β (6 mg/ml) were incubated on ice for 1 h with 0.37 mg/ml of the 19mer axin(383–401) peptide. Crystallization trials were conducted using MDL Structure Screen 1, in 2 µl hanging drop experiments. Unphosphorylated and tyrosine-phosphorylated GSK3β–axin peptide complexes yielded small crystals in several experiments. Conditions were optimized, and crystals large enough for data collection were obtained by mixing 1 µl of the tyrosine-phosphorylated GSK3β–axin peptide complex [6 mg/ml GSK3β + 0.37 mg/ml axin(383–401) in 25 mM HEPES–NaOH pH 7.0, 250 mM NaCl and 1 mM DTT] with 1 µl of precipitant containing 18% PEG 4000, 150 mM $MgCl_2$ and 100 mM Tris–HCl pH 7.5. Data to 2.4 Å were collected from a single crystal at 100 K on station ID29 (λ = 0.9253 Å) at the ESRF, and recorded on an ADSC Q4 CCD scanner. Images were integrated using MOSFLM (Leslie, 1995), and reduced and scaled using programs of the CCP4 suite (CCP4, 1994). The crystals had space group $P6_122$ or $P6_522$ with cell dimensions $a = b = 81.30$ Å, and $c = 283.70$ Å. The crystal volume was consistent with a solvent content of ~55% by volume, with one molecule in the asymmetric unit. The structure was solved by molecular replacement with the unphosporylated GSK3β structure (Dajani *et al*., 2001) (PDB code 1H8F) using AMoRe (Navaza, 1994), which resolved the space group as $P6_122$, and was refined using CNS (Brünger *et al*., 1998). Crystallographic statistics are given in Table II. The coordinates for the GSK3β–axin(383–401) complex have been deposited in the Protein Databank with accession code 1O9U. All molecular graphics were generated using PyMol (DeLano Scientific, San Carlos, CA, http://www.pymol.org).

Kinase assays

Kinase activities of GSK3β were determined using a phospho-primed peptide (GSM) derived from glycogen synthase, as previously described (Dajani *et al*., 2001; Fraser *et al*., 2002).

GSK3β-mutants and GST pull-down assay

GSK3β mutants were constructed as previously described (Fraser *et al*., 2002). [^{35}S]methionine-labelled GSK3β proteins (wild-type and mutant) were made using the TNT-coupled *in vitro* transcription/translation system according to the manufacturer's instructions (Promega). A 5 µl aliquot of each mix was removed and mixed with 20 µl of loading buffer to check the efficiency of the reaction. The remainder was split in half and mixed with purified GST fusion protein and 25 µl of washed glutathione–Sepharose beads (Amersham Pharmacia Biotech). This was made up to 250 µl with ice-cold 'NETN' buffer [100 mM NaCl, 0.5% NP-40, 20 mM Tris–HCl, pH 8.0, 1 mM EDTA supplemented with a Complete protease inhibitor tablet (Roche Molecular Biochemicals), 1 mM phenylmethylsulfonyl fluoride (PMSF) and 0.5 mM DTT]. Following incubation on a rotary mixer at 4°C for 1 h, samples were pelleted, washed three times with ice-cold buffer and analysed by SDS–PAGE and autoradiography.

Scaffolding factor determination

A 60 µg aliquot of purified β-catenin was pre-cleared with glutathione–Sepharose beads in NETN buffer for 30 min on a rotary mixer at 4°C. A 3 µg aliquot of this was incubated with the molar equivalent of purified GST proteins in a total of 50 µl for 18 h at 4°C. Glutathione–Sepharose beads (20 µl) and NETN buffer to a total volume of 250 µl were added. Samples were incubated on a rotary mixer at 4°C for 1 h, pelleted and washed three times with ice-cold buffer. Phosphorylation of the β-catenin substrate with or without GST was determined by incubation of the beads or the indicated amounts of purified His-tagged β-catenin with 10 µM recombinant GSK3β and 100 µM ATP in a total volume of 25 µl for 30 min at 30°C, in a buffer containing 50 mM HEPES pH 8.0, 12.5 mM $MgCl_2$, 2 mM DTT, 0.05 mM EDTA. The reaction was terminated by the addition of an equal volume of SDS loading buffer. Samples were analysed by SDS–PAGE and either silver stained or immunoblotted with anti-phospho β-catenin Ser33/37 Thr41 (Cell Signalling Technology) and anti β-catenin (Transduction labs).

Acknowledgements

We wish to thank Phillipe Meyer for assistance with data collection, David Barford and Adrian Harwood for stimulating discussions, and Benjamin Bax for making the coordinates of the GSK3β–FRAT complex available prior to general release. This work was funded by Cancer Research UK (L.H.P. and T.C.D.) and the Institute of Cancer Research Structural Biology Initiative (L.H.P.).

References

Bax,B. *et al*. (2001) The structure of phosphorylated GSK-3β complexed with a peptide, FRATtide, that inhibits β-catenin phosphorylation. *Structure*, **9**, 1143–1152.

Behrens,J., Jerchow,B.A., Wurtele,M., Grimm,J., Asbrand,C., Wirtz,R., Kuhl,M., Wedlich,D. and Birchmeier,W. (1998) Functional interaction of an axin homolog, conductin, with β-catenin, APC and GSK3β. *Science*, **280**, 596–599.

Bourne,Y., Watson,M.H., Hickey,M.J., Holmes,W., Rocque,W., Reed,S.I. and Tainer,J.A. (1996) Crystal structure and mutational analysis of the human CDK2 kinase complex with cell cycle-regulatory protein CksHs1. *Cell*, **84**, 863–874.

Brünger,A.T. *et al*. (1998) Crystallography and NMR system: a new software suite for macromolecular structure determination. *Acta Crystallogr. D*, **54**, 905–921.

Canagarajah,B.J., Khokhlatchev,A., Cobb,M.H. and Goldsmith,E.J. (1997) Activation mechanism of the MAP kinase ERK2 by dual phosphorylation. *Cell*, **90**, 859–869.

CCP4(1994) The CCP4 suite: programs for protein crystallography. *Acta Crystallogr. D*, **50**, 760–763.

Dajani,R., Fraser,E., Roe,S.M., Young,N., Good,V., Dale,T.C. and Pearl,L.H. (2001) Crystal structure of glycogen synthase kinase 3β: structural basis for phosphate-primed substrate specificity and autoinhibition. *Cell*, **105**, 721–732.

Ding,Y.N. and Dale,T. (2002) Wnt signal transduction: kinase cogs in a nano-machine? *Trends Biochem. Sci.*, **27**, 327–329.

Ferkey,D.M. and Kimelman,D. (2002) Glycogen synthase kinase-3β mutagenesis identifies a common binding domain for GBP and axin. *J. Biol. Chem.*, **277**, 16147–16152.

Frame,S., Cohen,P. and Biondi,R.M. (2001) A common phosphate binding site explains the unique substrate specificity of GSK3 and its inactivation by phosphorylation. *Mol. Cell*, **7**, 1321–1327.

Fraser,E. *et al*. (2002) Identification of the axin and Frat binding region of glycogen synthase kinase-3. *J. Biol. Chem.*, **277**, 2176–2185.

Hart,M.J., de los Santos,R., Albert,I.N., Rubinfeld,B. and Polakis,P. (1998) Downregulation of β-catenin by human axin and its association with the APC tumor suppressor, β-catenin and GSK3β. *Curr. Biol.*, **8**, 573–581.

Harwood,A.J. (2001) Regulation of GSK-3: a cellular multiprocessor. *Cell*, **105**, 821–824.

He,T.-C., Sparks,A.B., Rago,C., Hermeking,H., Zawel,L., da Costa,L.T., Morin,P.J., Vogelstein,B. and Kinzler,K.W. (1998) Identification of c-*MYC* as a target of the APC pathway. *Science*, **281**, 1509–1512.

Hsu,W., Zeng,L. and Costantini,F. (1999) Identification of a domain of axin that binds to the serine/threonine protein phosphatase 2A and a self-binding domain. *J. Biol. Chem.*, **274**, 3439–3445.

Ikeda,S., Kishida,S., Yamamoto,H., Murai,H., Koyama,S. and Kikuchi,A. (1998) Axin, a negative regulator of the Wnt signaling pathway, forms a complex with GSK-3β and β-catenin and promotes GSK-3β-dependent phosphorylation of β-catenin. *EMBO J.*, **17**, 1371–1384.

Itoh,K., Tang,T.L., Neel,B.G. and Sokol,S.Y. (1995) Specific modulation of ectodermal cell cell fates in *Xenopus* embryos by glocogen synthase kinase. *Development*, **121**, 3979–3988.

Leslie,A.G.W. (1995) *MOSFLM Users Guide*. MRC Laboratory of Molecular Biology, Cambridge, UK.

Li,L., Yuan,H.D., Weaver,C.D., Mao,J.H., Farr,G.H., Sussman,D.J., Jonkers,J., Kimelman,D. and Wu,D.Q. (1999) Axin and Frat1 interact with DvI and GSK, bridging Dvl to GSK in Wnt-mediated regulation of LEF-1. *EMBO J.*, **18**, 4233–4240.

Liu,C., Li,Y., Semenov,M., Han,C., Baeg,G.-H., Tan,Y., Zhang,Z., Lin,X. and He,X. (2002) Control of β-catenin phosphorylation/degradation by a dual-kinase mechanism. *Cell*, **108**, 837–847.

Murai,H., Okazaki,M. and Kikuchi,A. (1996) Tyrosine dephosphorylation of glycogen synthase kinase-3 is involved in its extracellular signal-dependent inactivation. *FEBS Lett.*, **392**, 153–160.

Navaza,J. (1994) AMoRE—an automated package for molecular replacement. *Acta Crystallogr. D*, **50**, 157–163.

Polakis,P. (2000) Wnt signaling and cancer. *Genes Dev.*, **14**, 1837–1851.

Seeling,J.M., Miller,J.R., Gil,R., Moon,R.T., White,R. and Virshup,D.M. (1999) Regulation of β-catenin signaling by the B56 subunit of protein phosphatase 2A. *Science*, **283**, 2089–2091.

Smalley,M.J. *et al*. (1999) Interaction of axin and Dvl-2 proteins regulates Dvl-2- stimulated TCF-dependent transcription. *EMBO J.*, **18**, 2823–2835.

Song,H.W., Hanlon,N., Brown,N.R., Noble,M.E.M., Johnson,L.N. and Barford,D. (2001) Phosphoprotein–protein interactions revealed by the crystal structure of kinase-associated phosphatase in complex with phosphoCDK2. *Mol. Cell*, **7**, 615–626.

Thomas,G.M., Frame,S., Goedert,M., Nathke,I., Polakis,P. and Cohen,P. (1999) A GSK3-binding peptide from FRAT1 selectively inhibits the GSK3-catalysed phosphorylation of axin and β-catenin. *FEBS Lett.*, **458**, 247–251.

Wodarz,A. and Nusse,R. (1998) Mechanisms of Wnt signalling in development. *Annu. Rev. Cell. Dev. Biol.*, **14**, 59–88.

Yanagawa,S., Matsuda,Y., Lee,J.-S., Matsubayashi,H., Sese,S., Kadowaki,T. and Ishimoto,A. (2002) Casein kinase I phsophorylates the Armadillo protein and induces its degradation in *Drosophila*. *EMBO J.*, **21**, 1733–1742.

Yost,C., Farr,G.H., Pierce,S.B., Ferkey,D.M., Chen,M.M. and Kimelman,D. (1998) GBP, an inhibitor of GSK-3, is implicated in *Xenopus* development and oncogenesis. *Cell*, **93**, 1031–1041.

Received September 19, 2002;
revised and accepted December 6, 2002